Chapter 3

Rigidization via Internal Resistive Heating

Rigidization of inflatable space structures via internal resistive heating requires carbon fiber reinforced material to consolidate and cure on-command. In terms of the spacecraft's life, the rigidization process transforms a structurally weak "balloon" into a robust, stable design. Internal resistive heating provides an active approach for inducing permanent shape-holding and structural stiffening and has been addressed extensively in Chapter 2. The use of internal resistive heating with feedback temperature control is applied to a novel, thermoset resin-coated carbon fiber composite. The material hardening initiated by Joule heating will be evaluated as a function of several curing parameters and compared to uncured material. A method for quantifying the change in material properties is experimentally measured through an instrumented test apparatus. The goal for this study is aimed to correlate the change in mechanical properties and resin curing to factors such as the curing temperature, curing time, and heating rate. Furthermore, the amount of increase in stiffness per unit of applied energy is also considered since internal resistive heating is traditionally an energy-expensive method.

This chapter addresses the issues and techniques associated with quantifying change in stiffness as a result of the curing process. First, the materials of interest (both the thermoset resin and reinforcing carbon fiber) are discussed. The primary experimental setups for measuring material stiffness are then described. Results of these tests are then presented and their significance is discussed.

3.1 Sample Composition and Preparation

The two components of the rigidizable material used throughout this study were a carbon fiber tow and an adjacent thermosetting epoxy resin. As discussed in Chapter 1, the idea behind CFRP composites is that a resin matrix can be used to transfer a load to the stronger, reinforcing fibers. The resin also provides fracture toughness, increased abrasion resistance, and corrosion and chemical resistance [1]. The combination of these two components results in a strong, tough material that has a high strength-to-weight ratio. In controlling when the change in material properties is triggered (through on-command rigidization), reinforced composites transform from initially flexible materials into stiff, durable materials. The specific carbon fiber and thermosetting resin selected for this study were chosen in order to balance mechanical strength with the ability to rigidize through resistive heating. The material properties of each component, as listed by their respective manufacturers, are shown in Table 3.1.

Table 3.1: Material properties for both the carbon fiber and thermosetting resin [4, 5].

Toho Besfight G40-800 12k Carbon Fiber		U-Nyet Set 201B Reactive Epoxy Binder	
Density (g/mL)	1.79	Viscosity (cP)	1200-2000
Fiber Count (dtex)	4200	Glass Transition Temperature (˚C)	62-65
Ultimate Tensile Strength (GPa)	5.58	Cured Glass Transition Temperature (˚C)	108-110
Tensile Modulus (GPa)	286	Onset of Cure (˚C)	100-120
Elongation (%)	1.95	Peak Cure Temperature (˚C)	150
Electrical Resistivity (Ω-cm)	0.0014	Particle Size (μm)	~200
Thermal Conductivity (W/mK)	10	Specific Gravity (g/mL)	1.2

A high strength, polyacrylonitrile (PAN)-based carbon fiber tow, Toho Besfight $G40-800$ (12k), was used to provide reinforcement to the thermosetting polymer. The fiber tow, which is electrically resistive in nature, also doubled as the internal resistive heating element for the composite. Compared to pitch-based graphite fibers, PAN-based tows provide increased ductility and higher resistivity. These two attributes were deemed appropriate for inflatable space structures hardened via resistive heating. The carbon fiber tow was coated with the resin using a dry powder "prepreg" system (DPPS) developed at Virginia Tech. In this procedure, uncoated tow is pulled from a spool and run through a tow-spreader at 15 ft/sec. This pneumatic device blows a focused stream of air across the fibers causing them to spread. The resin (in powder form) was then hand-sprinkled onto the "spread" fiber tow and the coated tow is then passed through a convection oven for 20 seconds at 175^{o}C in order to better adhere the resin particles to the fibers. Lastly, the

coated tow is then re-spooled for later use. It was determined that the mass fraction of the resin of the coated material ranged from $40 - 60\%$.

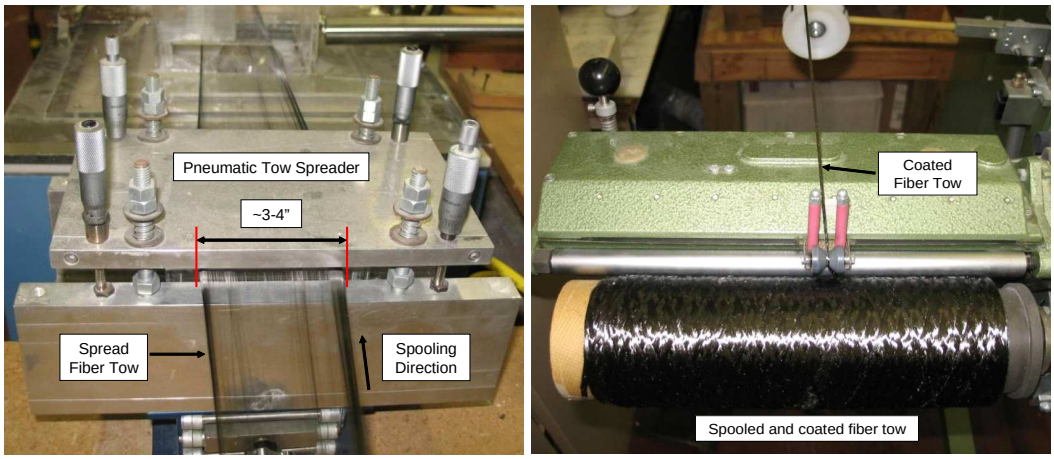

Figure 3.1: Spread tow line and re-spooled coated tow.

Two versions of the thermosetting resin, U-Nyte Set 201 Epoxy Binder, were investigated in this work. U-Nyte Set 201B, a phenoxy-toughened epoxy resin developed and supplied by Hydrosize Technologies, Inc., is a novel thermoset resin with a low curing temperature. As stated by Hydrosize, the onset of cure occurs between $100 - 120^oC$, with the maximum cure exotherm occuring at roughly 150^oC. This resin contains 97.2 wt% bisphenol A toughened epoxy, 2.6 wt% dicyandiamide, 0.2 wt% Amicure AMI-2 (a cure accelerator). U-Nyte Set 201A lacks the Amicure curing agent, which postpones the onset of curing to nearly 167^oC, and was developed in order to improve rheological properties for better processing. Previous work by researchers at Clemson [31] used ULTEM poly(etherimide) (PEI) thermosetting resin developed at GE Plastics. Comparatively, this resin offers many of the same advantages (high T_g, excellent thermal stability, and chemical resistance [48]) as the U-Nyte Set but requires a much higher curing temperature (380^oC). Since rigidization through internal resistive heating is an active technique, power is required to induce the material consolidation. Higher cure temperatures require larger amounts of power and possibly longer curing times.

3.1.1 Thermal Analysis on the Thermosetting Resins

Resin characterization tests performed in the Department of Chemistry at Virginia Tech on the U-Nyte Set resin experimentally measured the cure temperatures and viscosities of

both versions. Differential scanning calorimetry (DSC) was performed at heating rates of 5 and 10^{o}C/min in order to verify the curing temperature. This technique measures the heat released or absorbed by a material as a function of temperature. A TA Instruments AR1000 parallel plate rheometer was also used to measured resin viscosity versus temperature. These tests precluded work performed on rigidizing composites and proved valuable in subsequent cure profile designs.

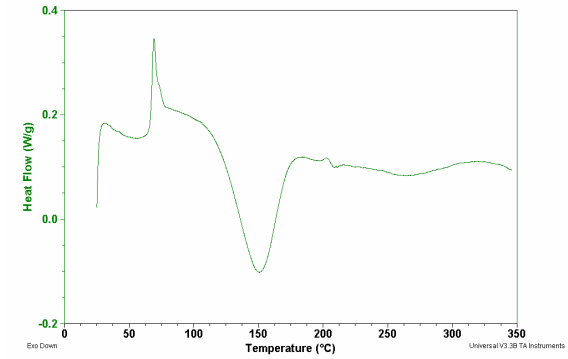

Figure 3.2: DSC measured on virgin U-Nyte Set 201B resin (exotherm down).

The first resin, U-Nyte Set 201B, experienced melting (the upward pointing "peak") as it passed from $70 - 90^o$C. This resin then demonstrated a cure exotherm (the large "valley") starting at about 100^{o}C and maximizing at a temperature of 150^{o}C. The adverse rheological behavior of the U-Nyte Set 201B resin, namely its inability to flow in the melt, was also witnessed with rheology testing. Specifically, this thermosetting material gelled (cured) before its viscosity could be reduced to a workable level and overall, never decreased below a gummy state.

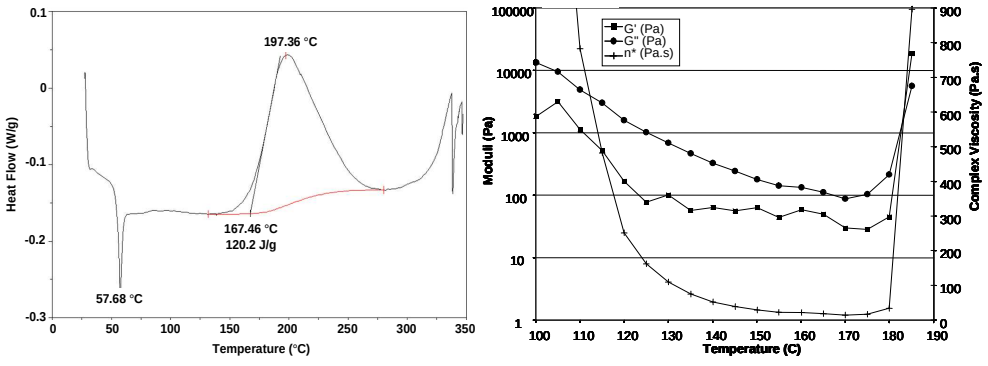

Figure 3.3: a. Cure temperature characterization results (exotherm up) on the U-Nyte Set 201A resin (left). b. Rheology results on this resin illustrate a significant increase in viscosity at a gel temperature of 180^{o}C (right).

Table 3.2: Summarized Thermosetting Resin Properties

Resin Type	Key Temperatures (°C)			Advantages	Disadvantages
	Melting	Cure Onset	Peak Curing Exotherm		
201A	50-60	167	197	More fluid-like in the melt	Has higher curing temperatures
201B	60-75	100	150	Lower curing temperature	Does not "flow" well in the melt

The DSC and rheology results (Figure 3.3) for U-Nyte Set 201A indicate that this resin begins to cure at 167^{o}C and reaches a maximum at a temperature of 200^{o}C. A minimum viscosity of 14 Pa·s was measured at 170^{o}C, and the gel point–when the system loses fluidity and the viscosity becomes very large [19]–was taken to be near 180^{o}C. Because this resin melts and flows well prior to curing, it offers the advantage of better consolidation around the reinforcing fibers.

The resin characterization results (summarized in Table 3.2) for both the U-Nyte Set 201A and 201B are later used to intelligently designed respective curing profiles. This topic is addressed in further detail in the Discussed of Results section.

3.2 Experimental Setup and Procedure

Rigidization of resin-coated, carbon fiber tow samples by internal resistive heating was experimentally validated and quantified through transverse bending tests. By applying a known deflection force to the sample, the deflection distance was measured and bending stiffness values were approximated. Specifically, a simple proof-of-concept deflection test and an improved, instrumented version were used in quantifying material rigidization.

3.2.1 Proof-of-Concept Stiffness Evaluation

Prior to temperature-controlled resistive heating, samples of a resin-coated fiber tow were heated with a manually-regulated voltage to see if internal resistive heating is a feasible method for inducing material consolidation. Samples coated in a similar U-Nyte Set 101 resin (which lacks the ability to cure) were heated and, although curing was not obtained using this resin, the test was performed to validate whether the heat generated through Joule heating of the fibers could be used to heat, melt, and cure a resin.

For this experiment, a 16.5cm (6.5in) coated sample was “strung” between two posts and its initial vertical deflection was marked. Then, a 149g mass was hung from the

midpoint of the sample and the resulting deflection was recorded. Following a resistive heating schedule, the undeflected and deflected (using the same mass) positions were again noted. It was desired to see that the vertical deflection under load was less for stiffer, post-heated samples. Two different samples were heated in an open-loop fashion (heating regimes are shown in Table 3.3) using a Xantrex XHR 300V-3.5A DC Power Supply to generate the voltage. The applied voltage was controlled manually during the heating process and temperatures were not measured. The results of this test are presented in the Discussion of Results Section.

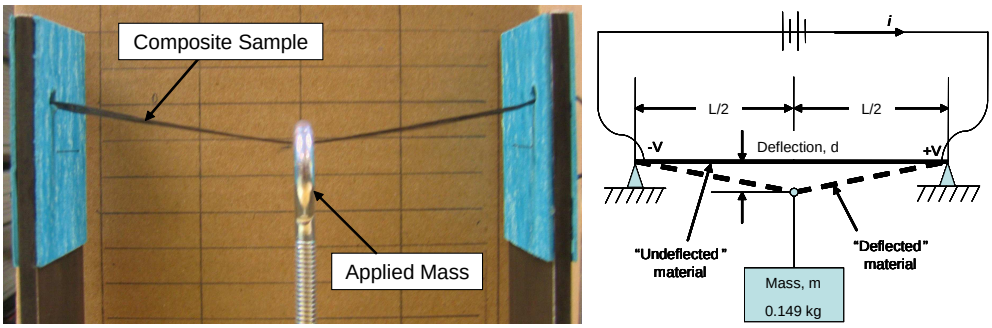

Figure 3.4: Experimental setup for measuring the bending stiffness of heated samples.

Table 3.3: Voltage potential and heating time for each sample.

Sample	Voltage Level (V)	Heating Time	
1	15	30	s
	14	2.5	min
2	15	30	s
	14	2.5	min

3.2.2 Instrumented Stiffness Measurement

Using the previously discussed (Chapter 2) internal resistive heating method with feedback temperature control, samples of the coated carbon fiber tow were subjected to a prescribed temperature profile. Again, samples ($15 - 20$cm in length) were fixed on each end and the voltage applied across each sample was controlled using a tuned proportional-integral (PI) controller that compared a measured sample temperature to the desired temperature. Verified through the use of infrared thermography, the maximum measured temperature (of all thermocouples) was used as the feedback signal and provided the best estimate of the core temperature of the sample.

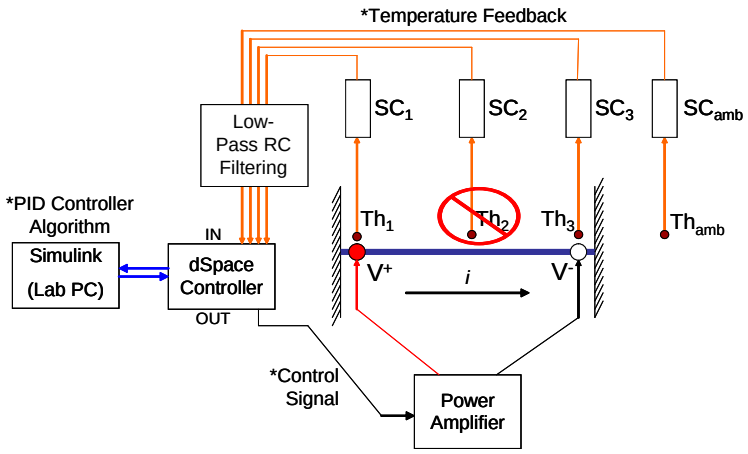

Figure 3.5: Two thermocouples were used to measure the sample temperature for full-scale rigidization testing.

Since the objectives of this test were to first cure the sample and then measure the hardened material's resulting stiffness, the positioning of the thermocouples was altered slightly. As with the initial proof-of-concept rigidization testing, the stiffness of the sample was again measured as a function of its resistance to transverse bending. For a sample fixed on each end and deflected at the midpoint along its length, even curing near the point of contact was crucial. Two 36-gauge, J-type thermocouples (placed at the ends) were used to record the sample temperature (Figure 3.5). Samples cured in this manner proved to be more consistently cured across their lengths and damage induced by a central thermocouple was negated.

An instrumented stiffness testing apparatus was constructed such that the deflection force and distance were measured continuously. With the sample clamped at the ends, a lead screw was used to manually "pull" the sample at its midpoint. The force of this "pull" was monitored by a 100g load cell (Transducer Techniques GSO-100) connected in series with the lead screw and pulling arm. A laser vibrometer (Polytec OFV 303 Sensor and OFV 3001 Controller) focused on the load cell was then used to detect the deflection incurred on the sample. Both of these signals were then input into dSpace and recorded for post-processing. During the actual test, the pulling arm was positioned such that the sample was initially untouched. When contact with sample was made, a force signal registered and the deflection distance was referenced to that instant.

Hardened samples were inserted into the test fixture such that the cure material spanned the distance between the end clamps (and also the width of the end clamps). This

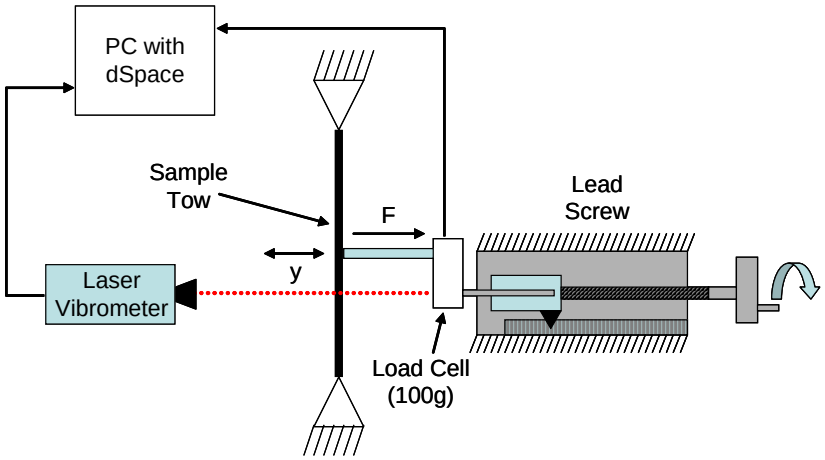

Figure 3.6: Instrumented design for measuring bending force and deflection.

prevented weaker, uncured areas of the samples from affecting the measured strength of the cured composite. The aluminum end clamps (Figure 3.7) sandwiched the composite material (roughly 1mm in thickness) at each end using four screws. Thin rubber sheeting was applied to the inner face on each half of the clamp. The rubber (a viscoelastic solid) formed around the composite as the clamps were tightened and prevented the sample from slipping. It also used to reduce "pinching" shear stress concentrations and minimize damage induced onto the sample by the clamps.

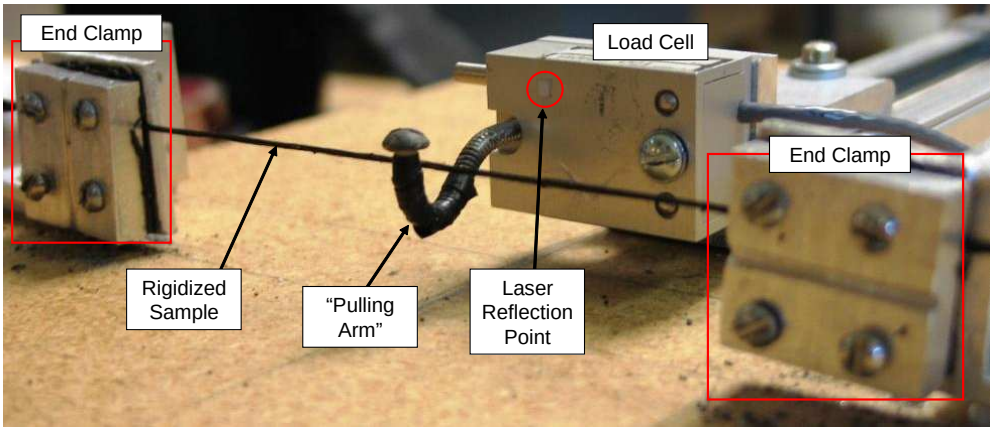

Figure 3.7: Instrumented test fixture shown with a hardened tow sample.

This test fixture was designed to quantify the change in stiffness of resin-coated, carbon fiber composites as a result of matrix consolidation through resistive heating. Factors in this process include the cure temperature, curing time, heating rate, and composite composition. Since the materials were prepared in a manner that included hand-sprinkling

resin powder onto the fiber tow, composition probably had the highest degree of variability. Using both versions of the U-Nyte Set epoxy resins, samples of each type were rigidized and their stiffnesses compared. A more in-depth study of one of the resins investigates sample stiffness and cure as a function of cure temperature, cure time, and heating rate conditions (Table 3.4). It was desired to determine how the cure energy expended as well as the time it took to conclude the heating schedule could be minimized while still achieving substantial stiffening.

Table 3.4: Curing parameter test matrix for samples coated with U-Nyte Set 201B resin.

Factor	Units	Tested Levels
Curing Temperature	˚C	50, 85, 100, 150, 200
Curing Time	min	0.5, 1, 2, 5, 10
Heating Rate	˚C/min	30, 45, 60, 90, 120

3.3 Discussion of Results

The results of the described tests investigate the use of internal resistive heating for causing material consolidation in thermoset-coated carbon fibers. Two methods were used to experimentally measure the change in material properties induced by the resistive heating process and correlate this stiffening effect to cure schedule parameters.

3.3.1 Initial Rigidization Tests

From the first experiment described, the vertical displacement due to mass loading was measured before and after resistive heating. The displacement values were estimated with the help of a background scale placed behind the fixed samples. Incremented with a 1.27cm (0.50in) vertical grid, the displacement values measured were accurate to about 0.32cm (0.125in). Prior to heating, the sample experienced a midpoint deflection of 1.59cm (0.625in) under loading. This "string-like" deflection created a sharp point in the deflection profile of the sample, as opposed to a continuous beam-like deflection. Plucking a guitar string would result in the same profile.

Through resistive heating, the resin particles melted and flowed around the fibers before cooling. The effect of this process was a decreased displacement under the same mass loading. The post-heated sample deflected only 1.27cm (0.50in), a 0.32cm decrease

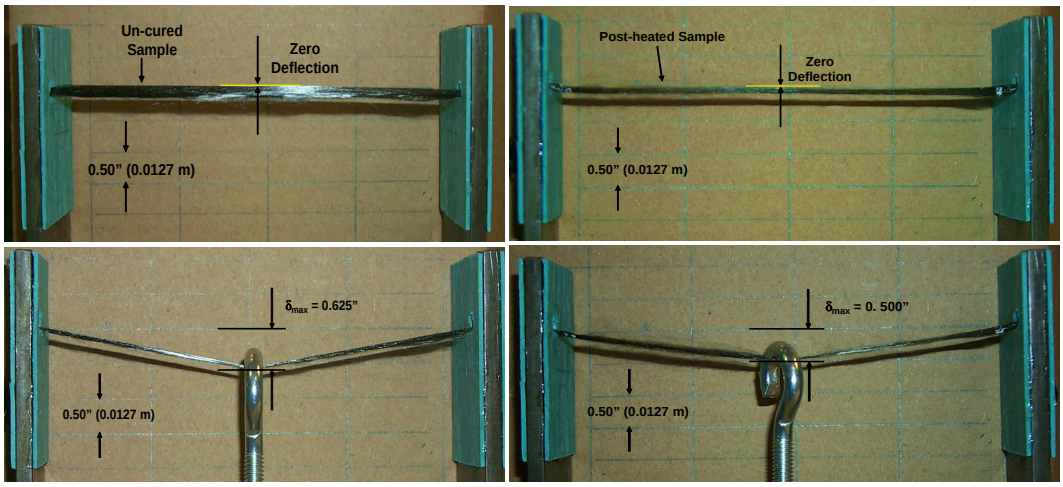

Figure 3.8: Undeflected and deflected composite sample prior to resistive heating (left) and the same sample after resistive heating (right).

compared to the unheated configuration. This procedure was repeated a second time on a new sample and the post-heated sample again deflected less, marking an increase in the material's bending stiffness.

Effective Stiffness Computations

Two modeling methods were considered for characterizing the increase in material stiffness of these samples. The first method modeled the samples as "pinned-pinned" Euler-Bernoulli beams, while the second technique described the samples as "fixed-fixed" strings. In the end, string theory was chosen to represent these materials, as their deflected shapes (Figure 3.8) lacked the continuous, cubic-like curvature required in beam theory. Specifically, string theory treats the samples as linear, elastic materials that possess no resistance to bending and whose measured vertical deflections result from stretching in the string.

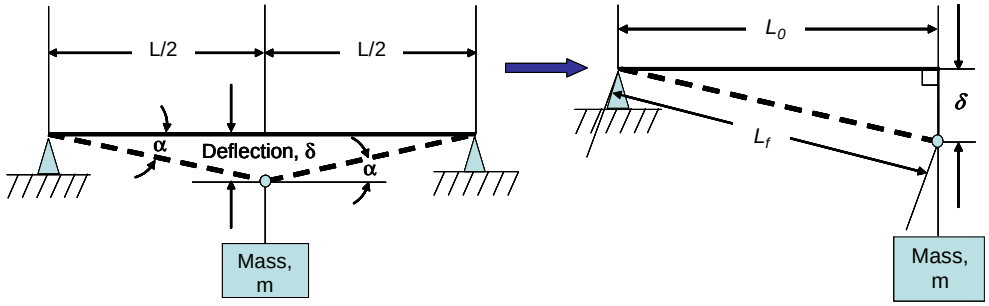

Figure 3.9: Deflected composite sample modeled as a string.

The deflection shape of a string with a force applied at the midpoint is a discontinuous function at the point of the applied load. The increase in length of the string permits it to be pulled away from an undeflected equilibrium. The "stretch" that existed within the string was assumed to be uniform throughout the length of the material and was caused by the tension generated in the material by the applied load. With the deflection occuring

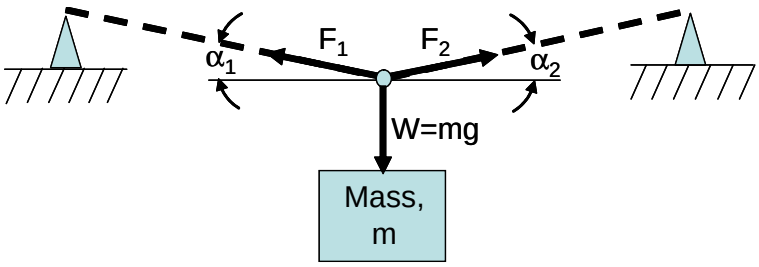

Figure 3.10: Tension forces, F_1 and F_2, arise within the material as a result of the applied load, W.

at the midpoint between the string ends, the angles of deflection, α, are equal and can be calculated by

$$\alpha = \tan^{-1}\left(\frac{\delta}{\mathrm{L_0}}\right) \tag{3.1}$$

where, L_0 is half of the sample's undeflected length, L. The stretched length, L_f, in the deflected state is computed using the Pythagorean's theorem for right triangles

$$L_f = \sqrt{L_0^2 + \delta^2}. \tag{3.2}$$

The tensile force, F, per unit cross-sectional area, A, results in a normal stress, σ, within the material.

$$\sigma = \frac{F}{A}. \tag{3.3}$$

Similarly, the corresponding strain within the material

$$\epsilon = \frac{L_f - L_0}{L_0} = \frac{\delta_L}{L_0} \tag{3.4}$$

is defined as the stretch, δ_L, per unit length, L_0, of the sample. Hooke's law [49] states that for linearly elastic, isotropic materials the stress generated in a material is directly proportional to the resulting strain,

$$\sigma = E\epsilon \tag{3.5}$$

where the material's modulus of elasticity, E, is the proportionality constant for this relationship. Combining expressions for stress and strain and substituting them into Hooke's

Law results in a new expression for the modulus of the material,

$$E = \frac{\sigma}{\epsilon} = \frac{FL_0}{A\delta_L}. \tag{3.6}$$

For materials rigidized by resistive heating, the elastic modulus of the hardened composite was expected to be greater than that of the pre-cured sample. However, Equation 3.6 demands that the cross-sectional area of the material be known. Since this value was small, not precisely known, and somewhat invariant over the length of sample, the hardening effect of the resistive heating was characterized by the material's restorative force,

$$F_R = EA = \frac{FL_0}{\delta_L}. \tag{3.7}$$

By eliminating area, A, from the equation, the resiliency of the material to the applied load was expressed in terms of the tensile force in the material, F, and the measured stretch, δ_L. If it is assumed that the change in area due to either the applied load (via Poisson's effect) or polymer consolidation shrinkage is negligible, the restorative force provides an alternative way of quantifying the material's change in stiffness. Except for the tensile force, all terms in Equation 3.6 are known. Summing the forces labeled in Figure 3.10 in the vertical direction yields

$$F_1 \mathrm{sin}\alpha_1 + \mathrm{F}_2 \mathrm{sin}\alpha_2 = \mathrm{W}. \tag{3.8}$$

where, due to symmetry, $F_1 = F_2$ and $\alpha_1 = \alpha_2$. Combining like terms and solving for F produces

$$F = \frac{W}{2\mathrm{sin}\alpha}. \tag{3.9}$$

Lastly, this expression can then be substituted into the previously derived equation (3.7) for restorative force

$$F_R = EA = \frac{WL_0}{2\delta_L \mathrm{sin}\alpha} \tag{3.10}$$

such that all terms on the right-hand-side are now known. The restorative force values were calculated for the measured vertical displacements of both samples. The resistive heating caused polymer melting and resulted in restorative force, F_R, values that were $2-2.5$ times that of the uncured sample value.

The dilemma in post-processing this data was that a rigidization process is designed to convert an initially flexible, "string-like" material into a stiff, rigid composite. String theory applied well to the pre-cured sample, though may not accurately depict model samples

Table 3.5: Calculated restorative forces for both samples before and after heating.

Sample	Material Condition	Measured Deflection, δ_0 (cm)	Deflection Angle, a ($^\circ$)	Stretched Length, L_f (cm)	Linear Strain, ε (cm/cm)	Calculated Tension, F N	Restorative Force, F_R N	Change in F_R %
1	pre-heat	1.59	10.8	8.46	0.0181	3.89	215.06	
1	post-heat	1.27	8.7	8.40	0.0116	4.84	416.03	93.45
2	pre-heat	1.75	11.9	8.49	0.0219	3.55	162.13	
2	post-heat	1.27	8.7	8.40	0.0116	4.84	416.03	156.60

with noticeable and measurable bending stiffness. These evaluations and this test fell short in predicting the precise amount of stiffness increase to be expected through rigidization via resistive heating. However, the test successfully demonstrated that the heat generated within the fibers through Joule heating was sufficient for heating the adjacent matrix. Further, both samples showed an increase in stiffness over their original states.

3.3.2 Temperature-Controlled Rigidization

The second round of resistive heating explored the rigidization of U-Nyte Set 201-coated, carbon fiber tow. Samples containing both the U-Nyte Set 201A and 201B resins were prescribed temperature profiles designed to fully cure and successfully stiffen the material. DSC was then used to verify cure and the described bending strength test fixture was used to quantify their rigidity. Tests aimed at identifying the effects that cure parameters such as the curing temperature, curing time, and heating rate have on the stiffness of the final product were then performed on samples coated in the U-Nyte Set 201B resin. The primary goal of this experiment was to relate resin curing to material stiffness. Ways to reduce the energy required to cure while still achieving effective material hardening were also gained from these results.

Mechanical Strength of Rigidization

A load cell and laser vibrometer were used to obtain force and deflection measurements for samples in transverse bending. These signals were analyzed so as to obtain stiffness values corresponding to a given curing profile. The procedure for quantifying stiffness and relating the strengths of the different samples is discussed. The "pulling" region of the data was indicated by increases in the load cell and laser vibrometer voltage signals. Likewise, the "releasing" or retracting of the sample was noted by when these signals returned to

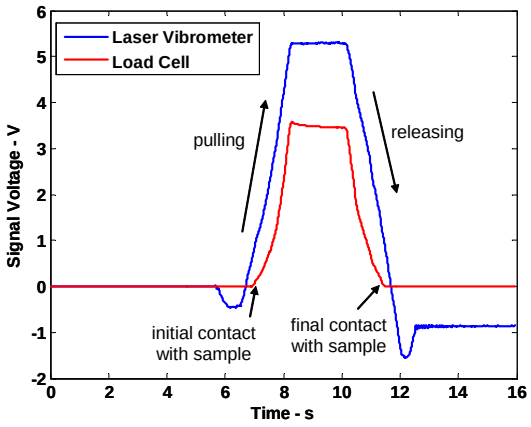

Figure 3.11: Raw data obtained from inducing transverse deflection at the midpoint of the fixed sample.

their original values. The raw data required additional post-processing in order to extract a force versus deflection relationship. First, the time at which the load cell first registered an increase in signal marked when the pulling arm contacts the sample. This time was defined as the starting time for the test and both signals were zeroed to mark change from this point. Secondly, the point at which the sample was no longer in a deflected state (at the end of the test) was marked and data occurring after this time was trimmed. The instrument sensitivities were then used to compute actual deflection and force values, such that the applied force could be plotted with respect to the induced displacement (Figure 3.12).

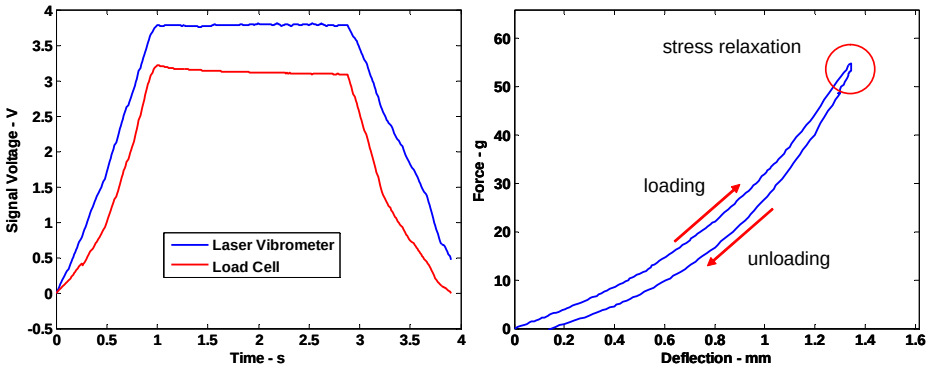

Figure 3.12: The remaining data only captured the deflected state of the sample (left). Hysteresis in the measurement appears when including the unloading data (right).

It is seen that when the deflection force returned to zero there exists some remaining

deflection in the sample, or hysteresis. Physically, this indicates that there was some non-conservative energy loss in the process. Two possible sources of hysteresis are viscoelastic behavior of the composite and slippage at the boundary conditions. Since the composite is partially polymer-based, and these materials behave visco-elastically [50], they exhibit stress relaxation over time for a constant applied strain. When sample is "pulled" out and held there, the polymer relaxes and the measured force required to deflect the sample this distance reduces. A second explanation of the hysteresis shown in Figure 3.12 is that the samples slipped from their fixed boundaries. If the end clamps allowed the material to moved, then causing a deflection in the sample would actually pull the material out of the clamps. Upon releasing the applied load, the sample now exists in a different state that before it was strained (as seen in the remaining deflection at zero load).

Ensuring that the clamps were securely tightened for each test minimized the slippage effect, though stress relaxation was not entirely avoidable in viscoelastic materials. Therefore, the evaluation of this data was restricted to the loading region of the full cycle. The relationship between the applied force and the resulting deflection is often transformed

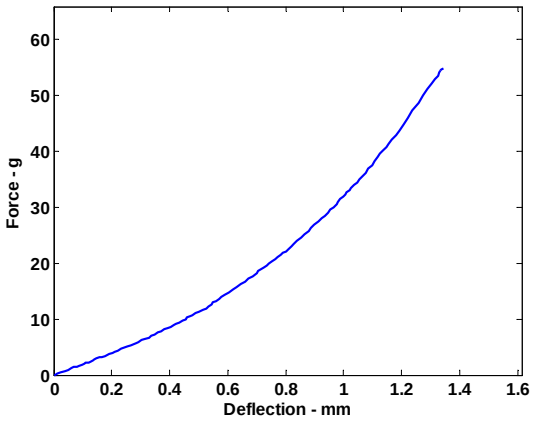

Figure 3.13: Typical force versus deflection data obtained for the transverse deflection of a rigidized sample.

into stress and strain values for a material such that the modulus of elasticity can be determined. In doing so, accurate knowledge of the sample dimensions (length, cross-sectional geometry) is required. For simplification and comparison purposes, the force and deflection data was kept in its original form. Variances in the material dimensions as well as an inability to accurately model the test (beam in bending or deflected string) further supported this technique. An effective stiffness, instead of a material modulus of elasticity, was determined

for these samples. For a Hookean spring, the spring stiffness is proportional to the force applied and inversely proportional to the incurred displacement. If the deflected samples are treated in this manner,

$$k_{eff} = \frac{F}{\delta}, \tag{3.11}$$

then the slope of the force versus deflection curve represents the material's bending "stiffness." For the samples to adhere to this assumption, linear relationships between force and deflection are required. Initial tests of cured composite samples, however, indicated that the force-deflection relationship was more accurately modeled as a quadratic relationship. Force-deflection data on a couple of representative samples emphasize this finding, as shown in Figure 3.14).

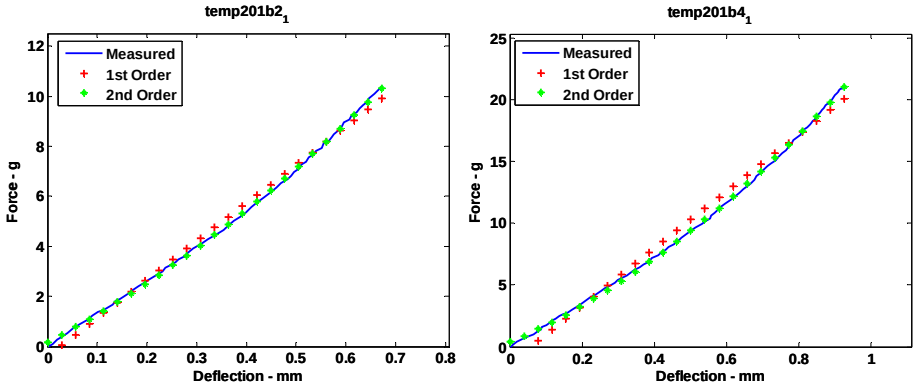

Figure 3.14: First and second-order polynomial fits were applied to force versus deflection data.

The quality of the first and second-order fits were evaluated by determining the mean square error

$$s^2 = \frac{\sum_{i}^{n} (y_i - \hat{y}_i)^2}{n-2}, \tag{3.12}$$

of the predicted values, $\hat{y}_i$, with respect to the measured values, y_i [51]. This measure of fit accuracy was then computed for the two data sets shown in Figure 3.14. The mean square error for the second-order, quadratic polynomial fits were found to be much smaller than for the first-order, linear fits.

The reduced mean square error values for the second-order fits necessitate their use in accurately approximating the force-deflection relationship. Two theories are introduced to explain the occurrence of this non-linearity. Since the materials heat from the inside out (as was shown through thermographic imaging), the highest degree of consolidation also

Table 3.6: Comparison of polynomial fits to describe the force-deflection data.

Sample	Order of Fit	Mean Square of the Error, s^2	Calculated Slope (g/mm)
temp201b2$_1$	1	0.0642	15.28
temp201b2$_1$	2	0.0057	18.86
temp201b4$_1$	1	0.5518	23.12
temp201b4$_1$	2	0.0247	29.90

occurs at the center of sample cross-section. Less-rigid outer fibers exist as a result of lower surface temperature and resin that migrates inwardly as it consolidates. When the sample was deflected, the pulling arm came into contact with the outer fibers first, possibly skewing the true deflection force and displacement data. Secondly, samples were placed into the test fixture without deliberately or evenly pretensioning them. Varying levels of tension within the samples may also be affecting the linearity of the data.

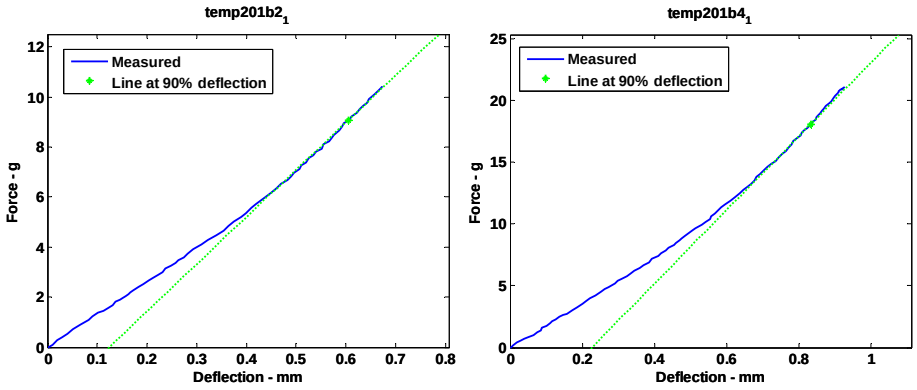

Figure 3.15: Instantaneous slopes were used to quantify the stiffness of a sample.

These effects diminish at larger deflections, producing a more linear force versus deflection curve. Stiffness values were extracted from the second-order polynomial fits by determining the slope of the force-deflection curve at 90% of maximum deflection (Table 3.6). Compared to the slopes of the linear approximations, the instataneous slopes are $15-20\%$ higher. This method was established in order to compare the rigidization successes of various curing profiles and the values reported have been obtained in this fashion.

3.3.3 Complete Curing of U-Nyte Set 201 Resin

Curing profiles designed from results of the thermal analysis performed on the U-Nyte Set resins were tailored so as to achieve full matrix consolidation and curing and maximum mate-

rial stiffness. Knowing that the 201A and 201B resins experience maximum cure exotherms at temperatures of 150^{o}C and 200^{o}C, respectively, these temperatures were selected as the cure temperatures for each sample type. In order to first melt and flow the resin before cure onset, an intermediate temperature of 85^{o}C was prescribed for 5 minutes. This temperature was also selected from the DSC results on each resin, as they both demonstrated melting above 70^{o}C and cure onset starting at about 100^{o}C. With the resin particles in a less-viscous state, the temperature was then ramped steadily (30^{o}C/min) to the cure temperature and held for 10 minutes prior to cooling.

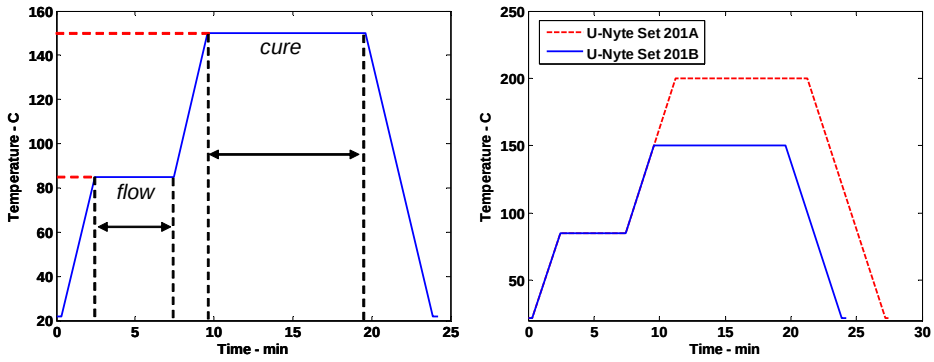

Figure 3.16: Typical curing profile (left) and specific profiles designed from DSC data on the U-Nyte Set resins (right).

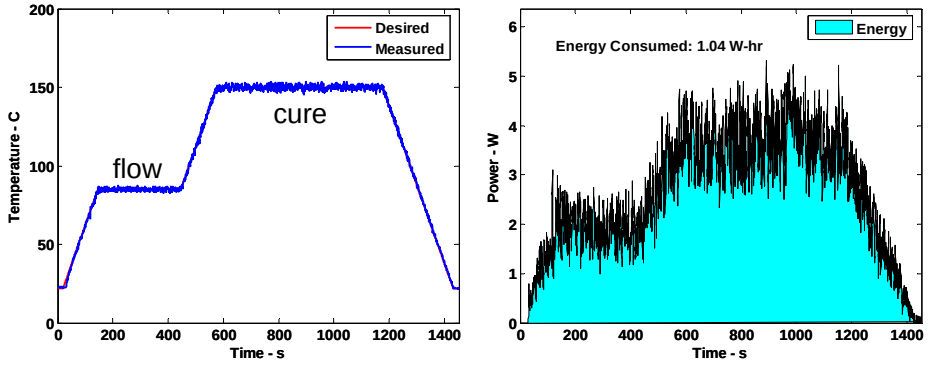

Figure 3.17: Actual temperatures measured during the cure of a U-Nyte Set 201B-coated sample (left). Electrical power and total consumed energy were also recorded for this process (right).

Samples coated with the U-Nyte Set 201B resin (containing the cure accelerator, Amicure AMI-2) were cured for 10 minutes at a temperature of 150^{o}C. The resin particles for this type of U-Nyte epoxy were ground with mortar and pestle in order to further aide

in the melting process. Since smaller particles have more surface area, and provided a more distributed resin phase, the resin melted fully in the 85^{o}C flow region (Figure 3.18). In the same manner, tow samples coated in the U-Nyte Set 201A resin also demonstrated melting/flowing when held at 85^{o}C.

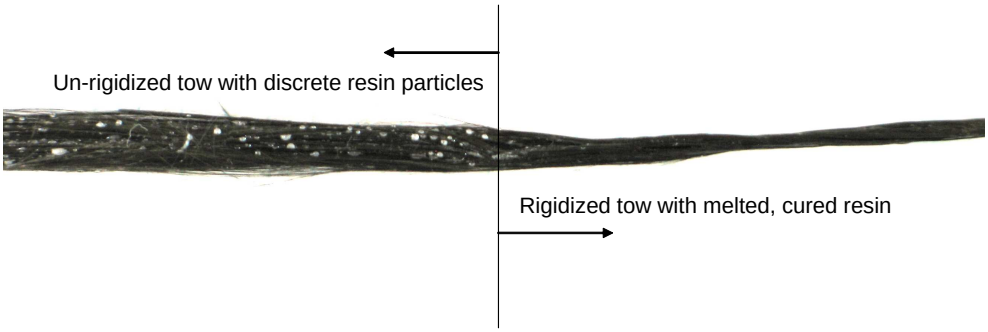

Figure 3.18: Incorporating a *flow* region into the temperature profile caused the U-Nyte Set resin particles to melt fully during their curing cycles.

The stiffness of the rigidized samples was then recorded for tow coated in both types of U-Nyte Set resin. Compared to the bending stiffness of uncured, coated tow, both sample types were many times $(16 - 20)$ stiffer (Figure 3.19). While these results indicate that the U-Nyte Set 201B-coated material produces stronger rigidized components, this type of resin is not necessarily better than the 201A form. Variability in resin particle size and coverage affects how well the resin surrounds the reinforcing fibers and possibly explains the difference in bending stiffness between sample types. Overall, both resistive heating cure profiles succeeded in causing significant increases in material rigidity.

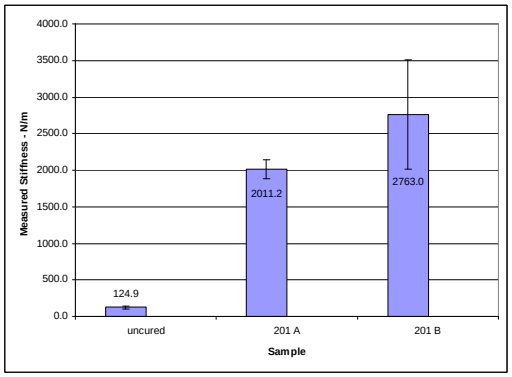

Figure 3.19: Bending stiffness comparison of rigidized tow samples.

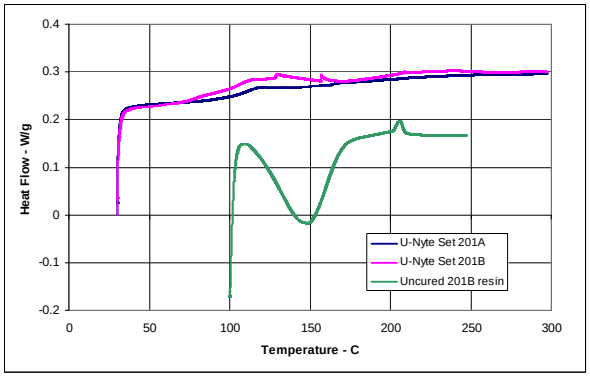

Figure 3.20: Post-rigidization DSC analysis indicates that both resins fully cured through resistive heating.

Since curing reactions give off heat (i.e. exothermic), any remaining uncured resin would be seen in performing DSC on the rigidized samples. Unlike the uncured 201B resin sample, DSC of the cured resin/fiber tow composites demonstrated no cure exotherms when heated from 30^oC to 300^oC. Figure 3.20 indicates that networks of cross-linking bonds were successfully formed during the resistive heating process and no remaining resin cured during the DSC test.

The prescribed temperature profile for samples coated with U-Nyte Set 201B required 1W-hr of energy for the 24-minute heating cycle. Factoring in the mass of a typical sample cured during these tests, the energy-density required by this process can be compared to the energy densities of several common power sources. Due to the lightweight

Table 3.7: Energy densities of common batteries and that required of this technique [6].

Battery Type	Energy Density (W-hr/kg)
Lead-acid	22
Nickel-cadmium (Ni-Cd)	44
Silver-zinc (Ag-Zn)	110
Sodium-sulfur (Na-S)	220
Lithium-sulftur (Li-S)	220
Iron-titanium hydride (Fe-Ti-H)	590
Magnesium hydride with Ni catalyst (Mg-H (Ni))	2300
U-Nyte Set 201B/carbon fiber composite	**8170**
Gasoline	13200

nature of carbon fiber composites and the high current draw of this material, significant energy per sample mass is required to induce rigidization and curing. The required energy density of the composite material is compared to the deliverable energy densities of some common battery types in Table 3.7. This type of evaluation allows the power source to be "sized" in relation to the amount of rigidizable material. For example, 14-kg iron-titanium

hydride (Fe-Ti-H) battery would be required to source the energy needed to rigidize 1-kg of the composite with the same curing profile. Power source selection, as well as minimizing the curing energy and time required to rigidize these materials, becomes especially important when considering their use for in-space operation. Furthermore, this comparison highlights the high-energy cost disadvantage of using internal resistive heating to cause material consolidation.

3.3.4 Cure Parameter Tuning for Successful Rigidization

Temperature-controlled resistive heating has been shown to cause significant material stiffening and complete resin curing in U-Nyte Set resin-coated fiber tow samples. The selection of the cure profile parameters (i.e. curing temperature, curing time, heating rate, flow temperature, etc.) was based on DSC analysis of the individual resins. While the prescribed profiles were "successful," can the heating schemes be further tuned to minimize electrical energy and time, while still producing stiff, fully-cured samples?

Narrowing the focus to one resin, the curing profile for samples coated in U-Nyte Set 201B resin was experimentally tuned. The curing temperature, curing time, and heating rate were investigated as possible sources for reducing the expended energy and time and still causing sufficient matrix consolidation and cure. As was shown in Figure 3.16, a similar curing profile was used that included the intermediate melting stage. Since the U-Nyte Set 201B resin lacks the ability to flow as well as the U-Nyte Set 201A resin, this stage incorporates additional time for it to melt prior to the onset of cure. Deeming this step vital to matrix consolidation required for composite rigidity, neither the flow temperature nor time at which the sample was held there were varied. In a similar fashion, typical cure profiles for epoxy resins included both time spent at an intermediate mold temperature as well as time spent with the material at a higher, cure temperature [42]. For processes (such as Resin Transfer Molding) in which a resin is cured under applied heat and pressure, the mold temperature is designed to reduce the resin viscosity and promote resin consolidation. Then, a period of time at the cure temperature establishes the final cross-linked material. In addition, it should be noted that the cooling period and/or cooling rate could be increased for additional cure energy and time savings. However, in this experiment, the heating rate and cooling rate were set equal.

Cure Temperature Study

First, the effect that cure temperature had on the cure of the U-Nyte Set 201B composite samples was investigated. Failure to meet the melting temperature ($70 - 90^oC$) would prohibit the resin particles from melting and flowing. If the cure onset temperature 120^oC is not met, then the melting resin would not form cross-linking bonds. The cure temperature also affects how quickly the cure rate happens, with the rate increasing at higher temperatures [19]. The trade off for quicker reactions comes at the increase in electrical energy required to produce higher temperatures, and the risk of resin decomposition at higher temperatures. Thermogravimetric analysis (TGA), which measures the weight loss of a material as a function of temperature, was performed on the U-Nyte Set 201B resin in order to determine its upper temperature limit. Marked by 5% weight loss, the U-Nyte

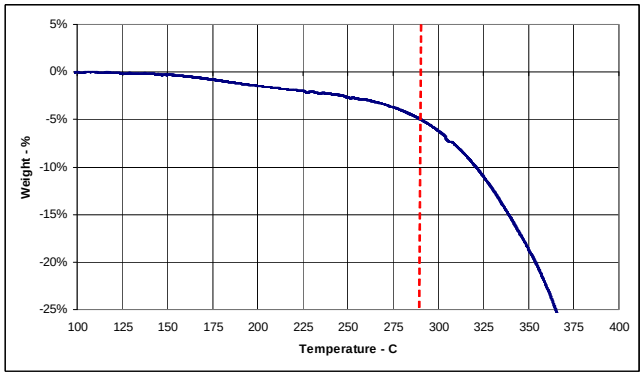

Figure 3.21: Resin weight loss measured as a function of temperature determines its userful range.

Set 201B resin resists degradation up to nearly 290^oC. This provides a temperature window substantially higher than the cure onset temperature and peak cure temperature of 120^oC and 150^oC, respectively.

This specific study was aimed at locating a cure temperature setting for carbon-fiber tow coated in a U-Nyte Set 201B resin that produces a cured, rigid composite. The cure temperatures that were tested spanned from 50^oC to 200^oC and were selected so as to illustrate both failed and successful selections. The cure time and heating (and cooling) rate were kept fixed at 10 minutes and 30^oC/min, respectively, and for cure temperatures higher than the 85^oC, 5 minutes of melting at the flow temperature was incorporated. One last sample, cured at 150^oC, but not held at the flow temperature, was heated in order emphasize to the need for resin consolidation.

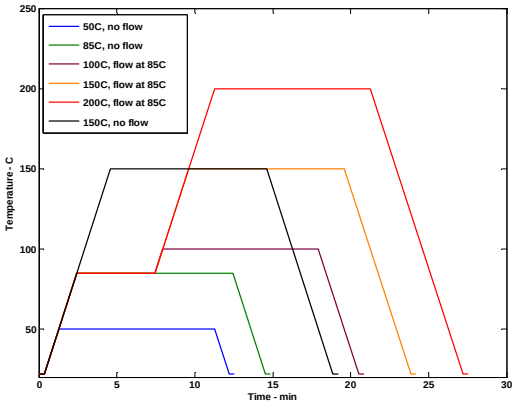

Figure 3.22: Heating schedules used to measure the effect of cure temperature on sample stiffness.

The stiffness of samples made from each cure profile in Figure 3.22 were then measured using the instrumented bending strength test fixture and their respective cure completions were evaluated with DSC testing. By performing thermal analysis of the "rigidized" samples, the appearance of a cure exotherm during the DSC testing would indicate that the sample did not fully cure during resistive heating.

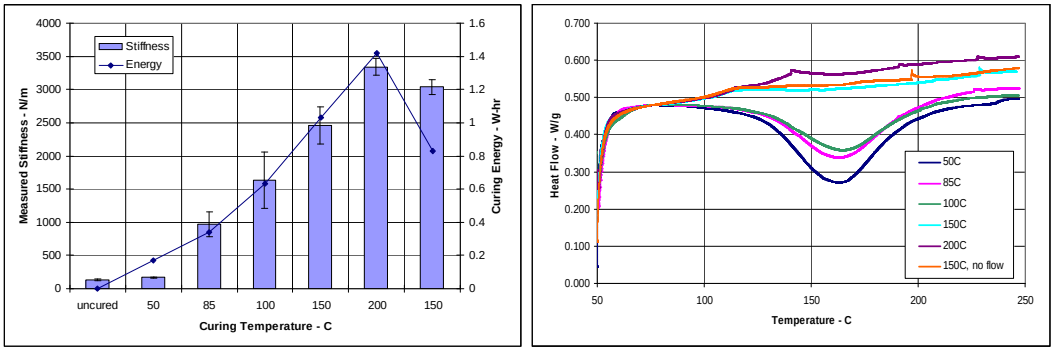

Figure 3.23: Stiffness and energy data (left) and DSC plots (right) for samples cured at various curing temperatures.

Stiffness and cure completion were used to gauge the effectiveness of curing this material at the various curing temperatures. In terms of the measured rigidity, it was expected that the sample could perform four different ways. First, the resin particles, if not heated sufficiently, would neither melt or cure. Samples matching this description would closely resemble the original flexible towpreg. Second, the resin could melt and flow when heated to its glass transition temperature. Some stiffening effect would result from the resin

consolidating around the fibers, but the sample would be weaker than for cross-linked resin. Third, a successful sample would both melt and cure during the heating process. Samples cured in this manner would be expected to experience the largest increase in material rigidity and contain fully-cured resin(Figure 3.24). Lastly, if heated too quickly, the resin could cure before it has a chance to melt. In this case, it would be expected to see completely cured resin in the DSC results but have stiffness values that were not as high.

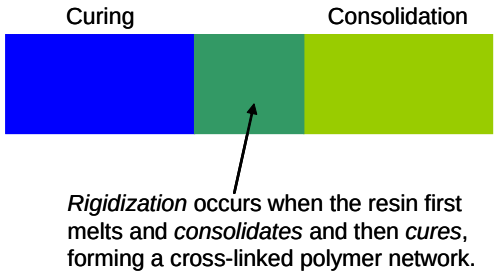

Figure 3.24: Successfully rigidizing composite materials requires a combination of consolidation and curing.

By creatively selecting the curing temperatures in this study, samples depicting each of these cure regions were produced (Figure 3.23). The sample that was cured at 50C neither melted, rigidized, or cured. The sample heated to 85^{o}C, did experience some melting which produced consolidation and rigidizing, but remained completely uncured. When heated to 100^{o}C, the sample again showed an increase in strength due to matrix consolidation. The DSC data for this sample shows a "shallower" curing exotherm, indicating that some of the material may have experienced localized curing during the resistive heating cycle. Samples heated to 150^{o}C and above, however, lacked cure exotherms in the thermal analysis, indicating that they fully cured. In addition, these samples demonstrated the largest increases in strength ($18 - 24$ times as strong as the uncured state). Sample 6, which was cured at 150^{o}C, also demonstrated that without a defined flow regime and at a heating rate of 30^{o}C/min, the resin still effectively consolidated before curing. This find allows quicker curing cycles and less energy to be spent, though with an increase in heating rate, the resin may need additional assistance in flowing before cure onset occurs.

These results have linked the curing temperature to both the resulting stiffness and cure completions for carbon fiber tow coated with U-Nyte Set 201B resin. For curing times of 10 minutes, the data suggests using a cure temperature of 150^{o}C or 200^{o}C in order to maximize cure completion and strength per amount of applied energy (Figure 3.25). It is

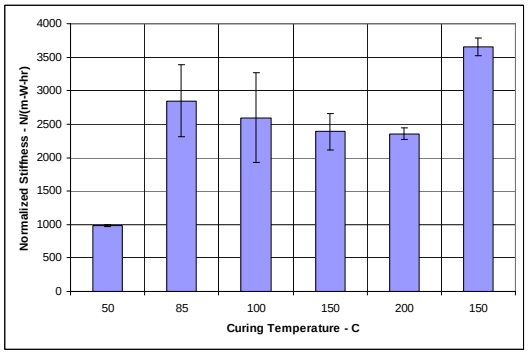

Figure 3.25: Normalized measured stiffness values with respect to expended energy.

possible to conceive that the samples could fully cure at a temperature of 100^{o}C, since this value roughly corresponds to the cure onset temperature, though much longer curing times would be required. It is important to note that if U-Nyte Set 201A resin were used, then the flow region added in to promote melting prior to cure onset could possibly be eliminated due to better rheological properties. Minus the flow region, the curing cycle would be shortened and less energy would be used.

Comparing to previous work using an ULTEM resin [31], which required more than 340W of peak power, these samples were fully cured and rigidized with the application of only $5 - 8$W of peak power and $1 - 1.4$W-hr of total electrical energy. Though the amount of material and test configuration were not equal, the reduction in curing temperature from 380^{o}C for the ULTEM to 150^{o}C for the U-Nyte Set is listed as a major factor in reducing the energy supplied to the material.

Curing Time Study

The amount of time that the sample was held at the curing temperature was also varied. It was advantageous to see if this variable could be minimized in order to reduce both electrical energy consumption and the overall processing time. Stiffness and DSC results on samples cured at 150^{o}C for 10 minutes validated this setting as both effectiving in rigidizing and curing the material. If this same temperature is again chosen as the curing temperature, what minimum amount of time can be used to still achieve adequate material rigidity as well as a complete resin curing? Building on the previous study, the test samples in this study were heated to 85^{o}C and held for 5 minutes, before being cured at 150^{o}C for varying

amounts of time (from 30 seconds to 10 minutes). The heating rate for this study was also maintained at 30^{o}C/min.

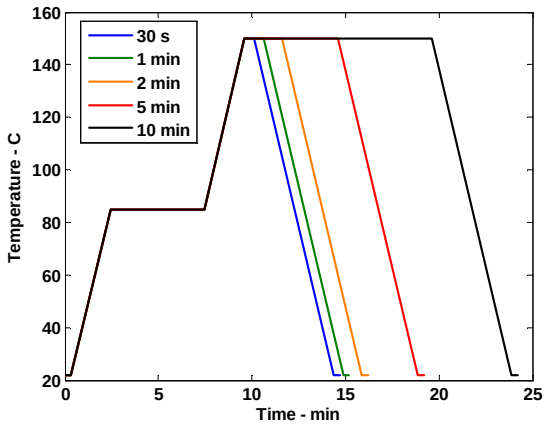

Figure 3.26: Heating schedules used to test the effect of curing time on the composite stiffness.

The expectations for this test were that there exists some lower curing time limit that can prescribed in order to still achieve fully cured samples. Since a setting of 10 minutes has been shown to rigidize successfully and cure completely, curing times less than this initial value were selected for investigation. As before, thermal analysis via DSC testing of the post-heated samples provides a qualitative measure of the cure completion for each sample.

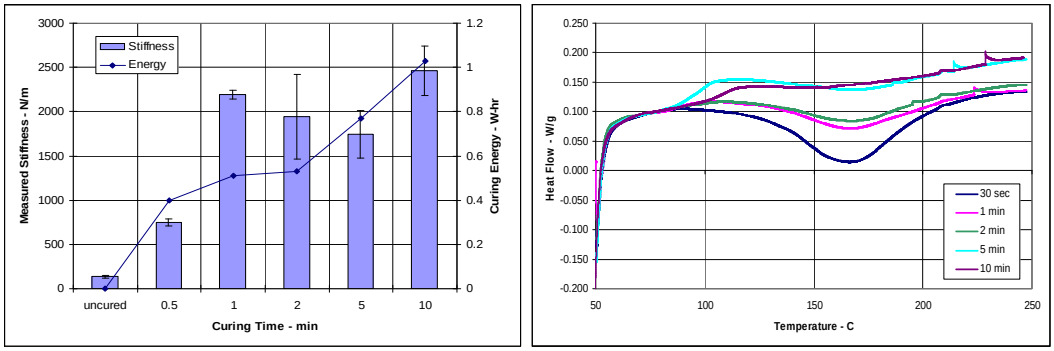

Figure 3.27: Measured stiffness (left) and DSC plots (right) for each sample.

Though samples cured for 1 minute or longer produced significant increases in stiffness, only samples that were cured for 5 minutes or longer fully cross-linked. The DSC plot demonstrates that the cure exotherm present in the first three samples becomes more shallow as curing time increases. Compared to the base curing profile, which included 10 minutes at 150^{o}C, this test asserts that curing the sample for half the time (5 minutes) will

produce roughly the same amount of stiffening and fully cure the resin matrix. By cutting the curing time in half, this process has been shortened and the total electrical energy was reduced from 1.0W-hr to 0.8W-hr, a 20% savings in both time and energy.

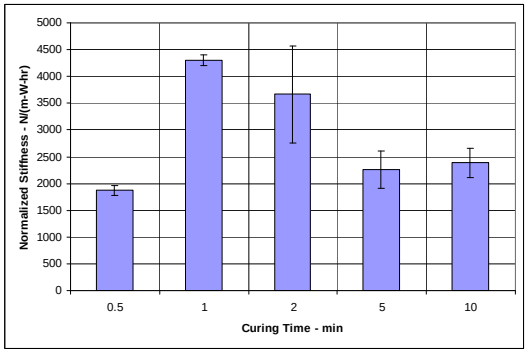

Figure 3.28: The cost of rigidization can be visualized by normalizing the stiffness values per applied electrical energy.

Again, the effectiveness of each curing profile (excluding cure completion analysis) is shown in a normalized stiffness plot. Though samples cured for $1-2$ minutes produced high stiffness per expended energy, only the samples that were cured for at least 5 minutes exhibit complete curing. It should be noted that this study is based on comparing the energy and time savings to the predefined base curing profile. These values do not depict the minimum energy that can be used to produced stiffened samples, but rather indicate how savings can be introduced into this curing process. Since curing rate increases with temperature, shorter cure periods are expected for higher curing temperatures. Further, the U-Nyte Set 201A resin, which offers a lower viscosity prior to cure onset, may not even require the additional flow region in this cycle.

Heating Rate Study

Lastly, the rate at which the material's temperature was increased and decreased during the curing profile was examined. The ability to shorten the total curing time for the sample also depends on how quickly the sample is heated and cooled. The baseline curing profile used a heating rate of 30^{o}C/min and provided adequate curing and rigidization. Increasing this parameter demands that both the material and the temperature control system can handle faster temperature changes. This study varied the heating rate in hopes of reducing the curing time and consumed energy required to cure U-Nyte Set 201B-coated fiber tow

at a temperature of 150^{o}C for 10 minutes.

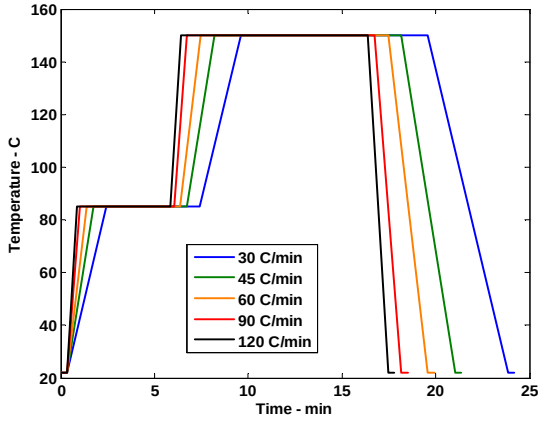

Figure 3.29: Samples were prescribed heating rates ranging from 30^{o}C/min to 120^{o}C/min in this study.

An "optimal" setting for the heating rate was not targeted, though this test illustrates the effect of increasing the heating rate for a given set of cure parameters and gauges the response speed of the resistive heating process. As before, sample was stiffness measured with the instrumented bending strength test fixture. DSC analysis of these samples were not performed on these samples since the samples were still cured for 10 minutes at 150^{o}C (which has already been shown to fully cure this resin).

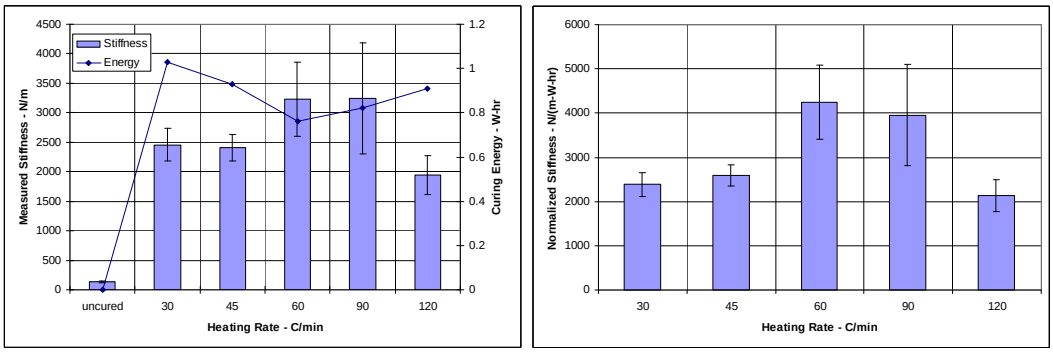

Figure 3.30: Measured stiffness and energy (left) along with normalized measured stiffnesses for samples cured at varying heating rates.

These results indicate that the heating rate of the process plays less of a role on the rigidized stiffness of the final product. By increasing this parameter from the original rate of 30^{o}C/min to 120^{o}C/min, however, the total time is reduced from 24.2 minutes to 17.8 minutes, a 26% savings. The electrical energy required is also lowered from 1.0W-hr to

roughly 0.9W-hr (10% less). For the heating rates attempted, the system also maintained accurate temperature tracking (Figure 3.31). This indicates that the system (i.e. material and thermocouples) can quickly respond to a faster tracking rate, further supporting the use of a higher heating rate.

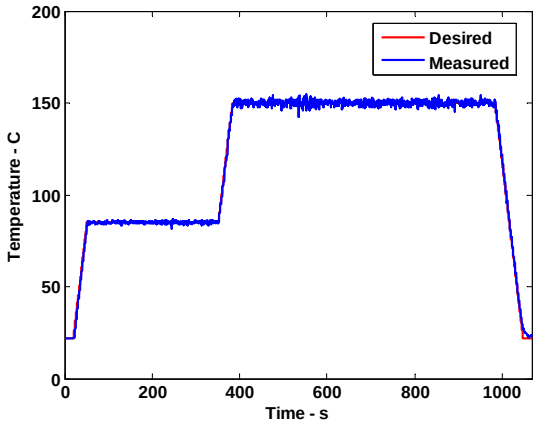

Figure 3.31: Measured and desired temperature signals for the maximum heating rate tested of 120^{o}C/min.

3.4 Conclusions

Rigidization via internal resistive heating of carbon fiber reinforced composites transforms composite material from an initially flexible state to one that can provide structural rigidity, permanent shape-holding, and durability. This chapter investigated the application of resistive heating to cause rigidization and matrix resin curing. Initial testing proved that the heat generated through uncontrolled resistive heating could be used to melt an adjacent polymer resin. Even without the ability to cross-link, the resin used during this testing (U-Nyte Set 101) demonstrated consolidation (melting and flowing) and resulted in measurably stiffer samples. Then, feedback temperature control (discussed in Chapter 2) was employed to prescribe accurate heating profiles for these materials. The resulting stiffness of samples heated in this fashion were quantified using an instrumented test fixture that measured bending force and deflection.

The primary goal of this chapter was to link, and yet differentiate, the concepts of resin curing and composite rigidization. In other words, does the presence of cured resin automatically infer rigidity or are other factors involved in transforming coated carbon fiber

from a flexible material into a structurally stiff element? Using DSC data for two U-Nyte Set resins (201A and 201B), curing profiles were designed to induce maximum curing and rigidization. Samples exposed to these heating profiles demonstrated successful rigidization (20 times stiffer than uncured material) and complete curing. The success of this test prompted a second investigation in which samples coated with U-Nyte Set 201B resin were subjected to heating profiles of varying cure temperature, curing time, and heating rates. Results of this round of testing indicate that the cure temperature is critical in determining whether or not the resin cures. Stiffening, a secondary effect, only happens when the resin melts and flows prior to cure onset. As a result, samples that were not heated to the cure onset temperature, or were not given ample opportunity to consolidate prior to curing were not as stiff. Studies on the curing time and heating rate accompanied this work and provided insight on how to obtain both rigidization and curing, while minimizing electrical energy and time.

It is important to note that an "optimal" curing profile was not obtained. Rather, a deeper understanding of how to prescribe temperature via electrical current/voltage control in order to cause physical changes in the material was gathered. Accordingly, the results of this work define rigidization as the sum of both material consolidation (melting and flowing) and polymer cross-linking (curing). In cases where either the consolidation or the curing requirement was deprived, the rigidity of the final product suffered.